Probability Density Function of Underwater Bomb Trajectory Deviation due to Stochastic Ocean Surface Slope

Peter C. Chu and Chenwu Fan
Naval Ocean Analysis and Prediction Laboratory
Naval Postgraduate School, Monterey, CA 93943

Kennard P. Watson
Naval Surface Warfare Center, Panama City, FL 32407

Corresponding Author: Peter C. Chu, Naval Ocean Analysis and Prediction Laboratory, Department of Oceanography, Naval Postgraduate School, Monterey, CA 93943
Tel: 1-831-656-3688, fax: 1-831-656-3686, email: pcchu@nps.edu, website: http://faculty.nps.edu/pcchu

Report Documentation Page

Form Approved
OMB No. 0704-0188

1. REPORT DATE	2. REPORT TYPE	3. DATES COVERED
2010		**00-00-2010 to 00-00-2010**

4. TITLE AND SUBTITLE	5a. CONTRACT NUMBER
Probability Density Function of Underwater Bomb Trajectory Deviation due to Stochastic Ocean Surface Slope	5b. GRANT NUMBER
	5c. PROGRAM ELEMENT NUMBER
6. AUTHOR(S)	5d. PROJECT NUMBER
	5e. TASK NUMBER
	5f. WORK UNIT NUMBER
7. PERFORMING ORGANIZATION NAME(S) AND ADDRESS(ES) **Naval Postgraduate School,Naval Ocean Analysis and Prediction Laboratory,Monterey,CA,93943**	8. PERFORMING ORGANIZATION REPORT NUMBER
9. SPONSORING/MONITORING AGENCY NAME(S) AND ADDRESS(ES)	10. SPONSOR/MONITOR'S ACRONYM(S)
	11. SPONSOR/MONITOR'S REPORT NUMBER(S)

12. DISTRIBUTION/AVAILABILITY STATEMENT
Approved for public release; distribution unlimited

13. SUPPLEMENTARY NOTES
Journal of Dynamic Systems, Measurement and Control, American Society of Mechanical Engineers, in press

14. ABSTRACT
Ocean wave propagation causes random change of ocean surface slope and in turn affects the underwater bomb trajectory deviation (r) through water column. This trajectory deviation is crucial for the clearance of obstacles such as sea mines or maritime improvised explosive device (IED) in coastal oceans using bombs. A nonlinear six degrees of freedom (6-DOF) model has been recently developed and verified at the Naval Postgraduate School with various surface impact speeds and surface slopes as model inputs. The surface slope (s) randomly changes between 0 and π/2 with a probability density function (PDF) p(s), or called the s-PDF. After s is discretized into I intervals by s1, s2, ?, si , ? sI+1, the 6-DOF model is integrated with a given surface impact speed (v0) and each slope si to get bomb trajectory deviation ?ir at depth (h) as a model output. The calculated series of {?ir } is re-arranged into monotonically increasing order (rj}. The bomb trajectory deviation r within (rj, rj+1) may correspond to one interval or several intervals of s. The probability of r falling into (rj, rj+1) can be obtained from the probability of s, and in turn the PDF of r, or called the r-PDF. Change of the r-PDF versus features of the s-PDF, water depth, and surface impact speed is also investigated.

15. SUBJECT TERMS

16. SECURITY CLASSIFICATION OF:			17. LIMITATION OF ABSTRACT	18. NUMBER OF PAGES	19a. NAME OF RESPONSIBLE PERSON
a. REPORT **unclassified**	b. ABSTRACT **unclassified**	c. THIS PAGE **unclassified**	**Same as Report (SAR)**	**28**	

Abstract

Ocean wave propagation causes random change of ocean surface slope and in turn affects the underwater bomb trajectory deviation (r) through water column. This trajectory deviation is crucial for the clearance of obstacles such as sea mines or maritime improvised explosive device (IED) in coastal oceans using bombs. A nonlinear six degrees of freedom (6-DOF) model has been recently developed and verified at the Naval Postgraduate School with various surface impact speeds and surface slopes as model inputs. The surface slope (s) randomly changes between 0 and $\pi/2$ with a probability density function (PDF) p(s), or called the s-PDF. After s is discretized into I intervals by $s_1, s_2, \ldots, s_i, \ldots s_{I+1}$, the 6-DOF model is integrated with a given surface impact speed (v_0) and each slope s_i to get bomb trajectory deviation $\hat{r}_i$ at depth (h) as a model output. The calculated series of $\{\hat{r}_i\}$ is re-arranged into monotonically increasing order (r_j}. The bomb trajectory deviation r within (r_j, r_{j+1}) may correspond to one interval or several intervals of s. The probability of r falling into (r_j, r_{j+1}) can be obtained from the probability of s, and in turn the PDF of r, or called the r-PDF. Change of the r-PDF versus features of the s-PDF, water depth, and surface impact speed is also investigated.

Keywords: 3D underwater bomb trajectory model, probability density function, bomb trajectory deviation, stochastic ocean surface slope, STRIKE35

1. Introduction

Movement of a fast-moving rigid body such as a bomb through water column has been studied recently [1-3]. These studies have been motivated by a new concept of using the Joint Direct Attack Munition (JDAM, i.e., 'smart' bomb guided to its target by an integrated inertial guidance system coupled with a global positioning system) Assault Breaching System (JABS) for mine/maritime improvised explosive device (IED) clearance, in order to reduce the risk to personnel and to decrease the sweep timeline without sacrificing effectiveness (Fig. 1). Underwater bomb trajectory depends largely on the surface impact speed and angle. When the surface impact of high-speed rigid body such as scaled MK-84 warhead is normal or near normal to the flat water surface, four types of trajectories have been identified from experimental and numerical modeling results [4] depending the characteristics of the warheads: with tail section and four fins (Type-1), with tail section and two fins (Type-1I), with tail section and no fin (Type-1II), and with no tail section (Type-IV). Type-1 trajectories are quite stable downward without oscillation and tumbling no matter the water entry velocity is high or low. Type-2 and Type-3 trajectories are first downward, then making 180^{o} turn (upward), and travel toward the surface. Type-IV trajectories are at first downward with little horizontal drift and then tumbling downward with large horizontal drift.

The horizontal distance (r) (or called trajectory deviation) between surface impact point and the bomb location varies with depth in different types of trajectories. This parameter draws attention to the naval research due to the threat of mine and maritime IED. Prediction of trajectory deviation of an underwater bomb contributes to the bomb breaching for mine and maritime IED clearance in surf and very shallow water zones

with depth shallower than 12.2 m (i.e., 40 ft), shallow water zones (12.2 – 91.4 m, i.e., 40-300 ft), and deep zones (deeper than 91.4 m, i.e., 300 ft) according to U.S. Navy's standards. The bombs' trajectory drift is required to satisfy the condition, $r \leq 2.1$ m, for the validity of mine clearance using bombs [5].

In coastal oceans, waves form when the water surface is disturbed, for example, by wind or gravitational forces. During such disturbances energy and momentum are transferred to the water mass and sea-state is changed. For very shallow and shallow water regions, the bottom topography affects the waves dramatically and causes a significant change in surface slope. When bomb strikes on the wavy ocean surface, a scientific problem arises: How does randomly changing ocean-surface slope affect the underwater bomb trajectory and orientation? Or what is the probability density function of the underwater bomb trajectory deviation due to random sea surface slope? The major task of this paper is to answer these questions. The effect of surface slope on the underwater bomb trajectory is presented in Section 2. Stochastic features of the sea slope are simply described in Section 3. A recently developed six degrees of freedom (6-DOF) model at the Naval Postgraduate School for predicting underwater bomb location and trajectory is depicted in Section 4. Ensemble 6-DOF modeling to get PDF of trajectory deviation d from the stochastically changing sea surface slope is described in Section 5. The conclusions are presented in Section 6.

2. Effect of Ocean Surface Slope on Underwater Bomb Trajectory

Let μ be the inclination angle of the ocean surface; and ϕ be the bomb impact angle relative to the normal direction of the ocean surface (Fig. 2). For a flat surface (no waves),

$$\mu = 0 \tag{1a}$$

For 90^o bomb striking (vertically downward),

$$\phi = 0 \tag{1b}$$

With ocean wave propagation, μ can be treated as an averaged value in a wave period; and corresponding averaged slope in a wave period (s) is given by

$$s^* = \tan \mu \,. \tag{2}$$

The ocean waves may cause evident slant of the ocean surface with $\mu \approx 55^o$ (Kinsman, 1965), which affects the underwater bomb trajectory, orientation, and horizontal drift (r) (Fig. 3). The differential effects depend on which part of the wave is impacted by the bomb (i.e., different sea slopes). Obviously, such a wave effect can be investigated by a 6-DOF model with a sloping surface (i.e., μ changing with time) and non-normal impact angle (i.e., $\phi \neq 0$).

Besides, the surface slope also affects the tail separation due to the bomb and cavity orientations and the air-cavity geometry. This is because the air cavitation or supercavitation is usually generated after the bomb enters the water surface [7]. The cavity is usually oriented in the same direction of the bomb velocity with its geometry simply represented by a cone with the angle (γ). The bomb orientation relative to the cavity is represented by the angle between the bomb main axis and velocity (β). The condition for bomb not hitting the cavity wall is given by (Fig. 4a)

$$\beta < \gamma \,. \tag{3a}$$

Violation of the condition (3) may cause the tail separation (bomb hitting the cavity wall), as shown in Fig. 4b. Ocean waves not only affect the bomb trajectory and orientation but also change the cavity orientation, which may cause

$$\beta > \gamma\,, \tag{3b}$$

i.e., the bomb may hit the cavity wall and cause the tail separation (Fig. 4).

3. PDF of Ocean Surface Slope

Wave height and wave period are approximately independent of each other for either wind waves or swells, but not for mixed waves. From mixed wave records, Gooda [8] found that there is a strong correlation between wave height and wave period. In fact, the correlation is mainly caused by the two or more groups of notable waves with different characteristic wave heights and periods in the mixed waves. With the independent assumption between wave amplitude and wave period (or wavelength), the PDF of averaged wave slope *s* scaled by its standard deviation σ (the real slope is s* = sσ) is obtained from the PDF of wave length and PDF of wave amplitude [9],

$$p(s) = \frac{n}{(n-1)}\, s\left[1 + \frac{s^2}{(n-1)}\right]^{-(n+2)/2}, \tag{4}$$

where *n* is the peakedness coefficient which is determined by both the spectral width of the gravity waves, and the ratio between the gravity wave mean-square slope and the detectable short wave mean-square slope. Generally speaking, the peakedness of slopes is generated by nonlinear wave–wave interactions in the range of gravity waves; and the skewness of slopes is generated by nonlinear coupling between the short waves and the underlying long waves. For *n* = 2, the PDF of the wavelength corresponds to the Rayleigh distribution. For *n* = 10, the PDF in (4) fits the Gram Charlier distribution [10], very

well in the range of small slopes. As $n \to \infty$, the PDF of the wavelength tends to the Gaussian distribution [9]. Fig. 6 shows four typical surface-slope characteristics: (a) n = 2, (b) n = 4, (c) n = 10, and n = 100. It is seen that There is almost no difference in PDF between n = 10 and n = 100.

4. A 6-DOF Model (STRIKE35)

Recently, a 6-DOF model has been developed at the Naval Postgraduate School for predicting underwater bomb location and trajectory. It contains three parts: momentum equation, moment of momentum equation, and semi-empirical formulas for drag, lift, and torque coefficients [11-13]. The momentum equation of a rigid body is given by

$$m\frac{d\mathbf{u}}{dt} = \mathbf{F}_g + \mathbf{F}_b + \mathbf{F}_d + \mathbf{F}_l\,, \tag{5}$$

where m is the mass of the rigid body, $\mathbf{u}$ is the translation velocity of the center of mass,

$$\mathbf{F}_g = -mg\mathbf{k}, \quad \mathbf{F}_b = \rho\Pi g\mathbf{k}, \tag{6}$$

are the gravity and buoyancy force; Π is the volume of the rigid body; $\mathbf{k}$ is the unit vector in the vertical direction (positive upward): and g is the gravitational acceleration. $\mathbf{F}_d$ is the drag force; and $\mathbf{F}_l$ is the lift force.

The moment of momentum equation is given by

$$\mathbf{J} \bullet \frac{d\mathbf{\Omega}}{dt} = -\sigma\mathbf{e} \times \left(\rho\Pi g\mathbf{k}\right) + \mathbf{M}_h, \tag{7}$$

where $\mathbf{\Omega}$ is the rigid-body's angular velocity vector; σ is the distance between center of volume (o_v) and center of mass (o_m), which has a positive (negative) value when the

direction from o_v to o_m is the same (opposite) as the unit vector **e**; $\mathbf{M}_h$ is the hydrodynamic torque due to the drag/lift forces; and **J** is the gyration tensor.

The drag/lift/torque coefficients should be given before running the 6-DOF model. These coefficients depend on various physical processes such as water surface penetration, super-cavitation, and bubble dynamics. A diagnostic-photographic method has been developed [4] to get semi-empirical formulae for calculating the drag/lift/torque coefficients for underwater bombs with dependence on the Reynolds number (Re), angle of attack (α), and rotation rate along the bomb's major axis (Ω) [4],

$$C_d = 0.02 + 0.35e^{-2\left(\alpha-\pi/2\right)^2}\left(\frac{\mathrm{Re}}{\mathrm{Re}^*}\right)^{0.2} + 0.008\Omega\sin\theta\,, \tag{8}$$

$$C_l = \begin{cases} 0.35\sin\left(\theta_1\right)\left(\dfrac{\mathrm{Re}}{\mathrm{Re}^*}\right)^{0.2} & \text{if } \alpha \le \dfrac{\pi}{2} \\ 0.1\sin\left(\theta_2\right) - 0.015\Omega\left(\dfrac{\mathrm{Re}}{\mathrm{Re}^*}\right)^2 \sin\left(\theta_2^{\,0.85}\right) & \text{if } \alpha > \dfrac{\pi}{2} \end{cases} \tag{9}$$

$$C_m = \begin{cases} 0.07\sin\left(2\alpha\right)\left(\dfrac{\mathrm{Re}^*}{\mathrm{Re}}\right)^{0.2} & \text{if } \alpha \le \dfrac{\pi}{2} \\ 0.02\sin\left(2\alpha\right)\sqrt{\left(\dfrac{\mathrm{Re}}{\mathrm{Re}^*}\right)} & \text{if } \alpha > \dfrac{\pi}{2} \end{cases} \tag{10}$$

Here, $\mathrm{Re}^* = 1.8\times10^7$, is the critical Reynolds number, and

$$\theta \equiv \left(\pi^{2.2} - \left(\pi - \left|\pi - 2\alpha\right|\right)^{2.2}\right)^{\frac{1}{2.2}} \mathrm{sign}\left(\pi - 2\alpha\right), \tag{11}$$

$$\theta_1 = \pi\left(\frac{2\alpha}{\pi}\right)^{1.8}, \quad \theta_2 = 2\pi\left(\frac{2\alpha}{\pi} - 1\right)^{0.7}. \tag{12}$$

5. PDF of Bomb's Horizontal Drift

Let the bomb be dropped in the vertical direction to the slanted sea surface characterized by an averaged slope ($s^* = \sigma s$) in a wave period, here $s^* = \tan \mu$ (see Fig. 1). Consider a 5-time of s* value as the interval [0, 5s*] for the change of the surface slope. This interval [0, 5s*] is divided into I equal sub-intervals,

$$\sigma s_i = \frac{5is^*}{I}, \quad i = 0,1,2,...,I\,, \tag{13}$$

with the corresponding inclination,

$$\mu_i = \arctan(\sigma s_i) = \arctan\frac{5is^*}{I}, \quad i = 0,1,2,...,I\,. \tag{14}$$

For a given parameter n in the s-PDF, the probability for s^* taking values between σs_{i-1} and σs_i is calculated by

$$P_i \equiv \text{Prob}(s_i \le s \le s_{i+1}) = \int_{s_i}^{s_{i+1}} p(s)ds\,. \tag{15}$$

The 6-DOF model is integrated I times (called ensemble integration) from the surface impact speed (V) and various μ_i values to get the bomb horizontal drift $\hat{r}_i$ (i = 0, 1, …, I) at depth $z = -H$. The series $\{\hat{r}_i,\ i = 0, 1, \ldots, I\}$ might not be in monotonically increasing or decreasing order. Therefore, it is reorganized into monotonically increasing order $\{r_j\,,\ j = 0, 1, \ldots, J\}$ with $J \le I$. The inequality is due to an interval $[r_j, r_{j+1}]$ of the horizontal drift corresponding to m intervals $\{[s_{i1}, s_{i1}+1],\ [s_{i2}, s_{i2}+1], \ldots, [s_{im}, s_{im}+1]\}$ of the surface slope (Fig. 7) . The probability for the bomb's horizontal drift r taking values between r_j and r_{j+1} is calculated by

$$Q_j \equiv \text{Prob}(r_j \le r \le r_{j+1}) = \int_{s_{i1}}^{s_{i1+1}} p(s)ds + \int_{s_{i2}}^{s_{i2+1}} p(s)ds + ... + \int_{s_{in}}^{s_{in+1}} p(s)ds\,. \tag{16}$$

The probability density between r_j and r_{j+1} is calculated by

$$p_j = \frac{Q_j}{r_{j+1} - r_j}. \tag{17}$$

From p_j, we can obtain the PDF of r, or called the r-PDF.

6. Sensitivity Studies

6.1 Dependence of the r-PDF on Depth

Dependence of r-PDF on depth can be identified from the ensemble integration (I = 100) of the 6-DOF model with given bomb's surface impact speed (V = 300 m/s), s^* = 0.2 (i.e., σ = 0.2), and n = 2 (i.e., large peakedness in the s-PDF). The calculated r-PDF (Fig. 8) is positively skewed for shallow depth (H = 12.2 m, i.e., 40 ft), reduces the skewness as depth increases to 50 m, becomes negatively skewed as the depth exceeding 91.4 m (i.e., 300 ft). The negative skewness strengthens as depth deeper than 91.4 m. The horizontal axis in all the panels Fig. 8 is the non-dimensional horizontal drift r/H. The median (50 percentile $q_{0.5}$) of the horizontal drift (r) is 0.16 m at the depth z = -12.2 m, 1.7 m at z = -50 m, 5.4 m at z = -91.4 m (300 ft), 18.0 m at z = -150 m, 34.0 m at z = -200 m, and 52.5 m at z = -250 m (Table 1). Here z is the vertical coordinates with z = 0 corresponding to the water surface. Thus, down to the depth of 50 m, the median value of the horizontal drift is always less than the Navy's criterion, i.e., 2.1 m. The 95 percentile ($q_{0.95}$) of the horizontal drift (r) represents a reasonable estimation (with 95% of confidence) of the distance between bomb and mine/maritime IED when the bomb maneuvering in the water column. If this value is smaller than 2.1 m, according to the Navy's standard, the bomb will effectively 'kill' the mine/maritime IED. It is 0.32 m at the depth z = -12.2 m, 2.8 m at z = -50 m, 7.86 m at z = -91.4 m (300 ft), 22.5 m at z =

-150 m, 40.0 m at z = -200 m, and 60.0 m at z = -250 m (Table 2). The 5 percentile ($q_{0.05}$) of the horizontal drift (r) represents the minimum distance (likely) between bomb and mine/maritime IED when the bomb maneuvering in the water column. It is 0.13 m at the depth z = -12.2 m, 0.6 m at z = -50 m, 5.48 m at z = -91.4 m (300 ft), 10.5 m at z = -150 m, 24.0 m at z = -200 m, and 40.0 m at z = -250 m (Table 3).

6.2. Dependence of the *r*-PDF on the Peakedness of the *s*-PDF

Keeping all the initial conditions in running the 6-DOF model the same as described in subsection 6.1 except changing the parameter n of the s-PDF from 2 to 100 (small peakedness), the ensemble integration of the 6-DOF model shows the following results. The calculated r-PDF (Fig. 9) is almost zero skewness for shallow depths (H = 12.2 m, 50 m), becomes negatively skewed as the depth of 91.4 m (i.e., 300 ft). The negative skewness strengthens as depth deeper than 91.4 m. Comparing between Fig. 9 and Fig. 8, we may find that the negative skewness of r-PDF increases as n increases. The median, $q_{0.95}$, and $q_{0.05}$ of the horizontal drift (r) do not change too much as n increases from 2 to 100 (Tables 1-3).

6.3. Dependence of the *r*-PDF on the Averaged Surface slope σ

Keeping all the initial conditions in running the 6-DOF model the same as described in subsection 6.1 except increasing the averaged surface slope σ from 0.2 to 1, the calculated r-PDF (Fig. 10) is negatively skewed at all depths; and the negative skewness enhances as the depth increases. Comparing between Fig. 10 and Fig. 8, we may find that the negative skewness of r-PDF increases as σ increases. The median, $q_{0.95}$, and $q_{0.05}$ of the horizontal drift (r) increase drastically as σ increases from 0.2 to 1.0 (Table3 1-3). For example, $q_{0.95}$ is 0.54 m at depth z = -12.2 m, 4.0 m at z = -50 m, 10.05

m at z = -91.4 m (300 ft), 25.5 m at z = - 150 m, 46.0 m at z = -200 m, and 67.5 m at z = -250 m (Table 2).

6.4. Dependence of the *r*-PDF on the Surface Impact Speed *V*

Keeping all the initial conditions in running the 6-DOF model the same as described in subsection 6.1 except decreasing the surface impact speed *V* from 300 m/s to 200 m/s, the calculated *r*-PDF (Fig. 11) is quite comparable to case with the impact speed of 300 m/s (Fig. 8) such as positive skewness for shallow depth (*H* = 12.2 m, i.e., 40 ft), weaker skewness as depth increasing to 50 m, negative skewness as the depth exceeding 91.4 m (i.e., 300 ft). Comparing between Figs. 11 and 8, reduction of surface impact speed leads to the increase of the peakedness of the *r*-PDF. The median, $q_{0.95}$, and $q_{0.05}$ of the horizontal drift (*r*) are usually higher for *V* = 200 m/s than that for *V* = 300 m/s except for the very shallow water depth (z = -12.2 m) where $q_{0.95}$, and $q_{0.05}$ are lower for *V* = 200 m/s (0.17 m, 0.04 m) than that for *V* = 300 m/s (0.32 m, 0.13 m) (Tables 1-3).

7. Conclusions

The PDF of the horizontal drift of underwater bomb trajectory (i.e., *r*-PDF) due to stochastic ocean surface slope is obtained through ensemble integration of the 6-DOF model recently developed at the Naval Postgraduate School. For a bomb dropping in the vertical direction to a slanted sea surface, the input parameters of the 6-DOF model are the bomb's surface impact speed (*V*), and surface slope. The surface slope is a random variable depending on two parameters: (a) averaged slope within a wave period (σ), and (b) peakedness of the *s*-PDF (*n*). The s-PDF is discretized into *I* intervals (in this paper, *I* = 100). For given values of (*V*, σ, *n*), the 6-DOF model is integrated *I* times with different values of the surface slope from the *s*-PDF to obtained *I* values of the horizontal

drift at various depth. The *r*-PDF is then constructed from these *r* values. The r-PDF has the following features:

(1) The *r*-PDF varies with depth. Usually, the *r*-PDF is positively skewed for very shallow water (H = 12.2 m, i.e., 40 ft), and negatively skewed down below. Increase of the peakedness parameter of the *s*-PDF (n) or the averaged surface slope in a wave period (σ) reduces the positive skewness at the very shallow water and enhances the negative skewness. Decrease of the bomb's surface impact speed (V) enhances the peakedness of the *r*-PDF. Three measures were calculated ($q_{0.05}$, $q_{0.5}$, and $q_{0.95}$) from the *r*-PDF.

(2) The values of $q_{0.95}$ are small for all cases at a very shallow depth (z = -12.2 m, i.e., 40 ft) with a maximum value of 0.54 m for the initial conditions of (V = 300 m/s, n = 2, σ = 1.0). This value (0.54 m) is much smaller than the critical value of 2.1 m for effectively 'killing' the mine/maritime. This may prove that the Joint Direct Attack Munition (JDAM) Assault Breaching System (JABS) is effective to clear mines and light obstacles in very shallow water (depth up to 12.2 m, i.e., 40 ft).

(3) The values of $q_{0.95}$ are all larger than 2.1 m when the depth deeper than 50 m. This indicates that to extend the JABS from very shallow water (12.2 m depth) to shallow water (12.2 m – 91.4 m) needs more studies.

Acknowledgments

The Office of Naval Research Breaching Technology Program (Grant Number: N0001410WX20165, Program Manager: Brian Almquist) supported this study.

References

[1] Chu, P.C., and G. P. Ray, 2006, "Prediction of high-speed rigid body maneuvering in air-water-sediment," *Adv. Fluid Mech.*, **6**, edited by M. Rahman and C.A. Brebbia, WIT Press (ISBN-1-84564-163-9), 43-52.

[2] Ray G. P., 2006. *Bomb Strike Experiments for Mine Clearance Operations*. MS Thesis in Meteorology and Physical Oceanography, Naval Postgraduate School, Monterey, California, pp. 197.

[3] Chu, P.C., Fan, C.W., and Gefken, P.R., 2008, "Semi-empirical formulas of drag/lift coefficients for high-speed rigid body maneuvering in water column," *Adv. Fluid Mech.*, **7**, edited by M. Rahman and C.A. Brebbia, WIT Press (ISSN-1743-3533), 163-172.

[4] Chu, P.C., Fan, C.W., and P. R. Gefken, 2010. "Diagnostic-photographic determination of drag/lift/torque coefficients of high speed rigid body in water column," *ASME J. Appl. Mech*., **77**, 011015-1- 011015-15.

[5] Humes, G., 2007. *Technology Transition Agreement, EC SHD-FYO6-03 FNC Product: Standoff Assault Breaching Weapon Fuze Improvement*. pp.10.

[6] Kinsman, B., 1965, *Wind Waves*, Prentice-Hall Inc., Englewood Cliffs, New Jersey, Library of Congress Catalog Card Number: 64-10136, pp. 676.

[7] Dare, A., Landsberg, A., Kee, A., and Wardlaw, A., 2003, "Three-dimensional modeling and simulation of weapons effects for obstacle clearance," *DoD User Group Conf*., Bellevue, Washington, 09-13 June, pp. 9.

[8] Gooda, Y., 1977, "The analysis on the joint distribution of period and wave height from the records of wave observations (in Japanese)," *Technol. Res. Data Estuaries,* **272,** 1–19.

[9] Liu, Y., Yan, X.-H., Liu, W.T., and Hwang, P.A., 1997, "The probability density function of ocean surface slopes and its effects on radar backscatter," *J. Phys. Oceanogr*., **27**, 782-797.

[10] Cox, C. S., and Munk, W. H., 1954, "Measurement of the roughness of the sea surface from photographs of the sun's glitter," *J. Opt. Soc. Amer.,* **44,** 838–850.

[11] Chu, P.C., and Fan, C.W., 2006. "Prediction of falling cylinder through air-water-sediment columns," *AMSE J. Appl. Mech*., **73**, 300-314.

[12] Chu, P.C., and Fan, C.W., 2007, "Mine impact burial model (IMPACT35) verification and improvement using sediment bearing factor method," *IEEE J. Ocean. Eng.*, **32** (1), pp. 34-48.

[13] Chu, P.C., 2009, "Mine impact burial prediction from one to three dimensions," *ASME Appl. Mech. Rev*., **62** (1), 010802 (25 pages), DOI: 1115/1.3013823.

Table 1. The median horizontal drift (unit: m) of an underwater bomb at various depths obtained from ensemble integration of the 6-DOF model with various input parameters.

Depth (m)	Case 1: V = 300 m/s n = 2 σ = 0.2	Case 2: V = 300 m/s n = 100 σ = 0.2	Case 3: V = 300 m/s n = 2 σ = 1.0	Case 4: V = 200 m/s n = 2 σ = 0.2
12.2	0.16	0.16	0.37	0.17
50.0	1.7	1.8	3.1	2.5
91.4	5.4	5.7	8.6	8.9
150.0	18.0	18.0	22.5	25.5
200.0	34.0	34.0	42.0	44.0
250.0	52.5	55.0	62.5	65.0

Table 2. The values of $q_{0.95}$ for the horizontal drift (unit: m) of an underwater bomb at various depths obtained from ensemble integration of the 6-DOF model with various input parameters.

Depth (m)	Case 1: V = 300 m/s n = 2 σ = 0.2	Case 2: V = 300 m/s n = 100 σ = 0.2	Case 3: V = 300 m/s n = 2 σ = 1.0	Case 4: V = 200 m/s n = 2 σ = 0.2
12.2	0.32	0.27	0.54	0.17
50.0	2.8	2.55	4.0	3.6
91.4	7.86	7.40	10.05	10.97
150.0	22.5	21.0	25.5	28.5
200.0	40.0	38.0	46.0	48.0
250.0	60.0	60.0	67.5	70.0

Table 3. The values of $q_{0.05}$ for the horizontal drift (unit: m) of an underwater bomb at various depths obtained from ensemble integration of the 6-DOF model with various input parameters.

Depth (m)	Case 1: V = 300 m/s n = 2 σ = 0.2	Case 2: V = 300 m/s n = 100 σ = 0.2	Case 3: V = 300 m/s n = 2 σ = 1.0	Case 4: V = 200 m/s n = 2 σ = 0.2
12.2	0.13	0.05	0.15	0.04
50.0	0.6	0.80	1.8	1.05
91.4	5.48	7.40	5.76	5.30
150.0	10.5	12.45	18.0	18.0
200.0	24.0	26.0	34.0	32.0
250.0	40.0	45.0	55.0	55.0

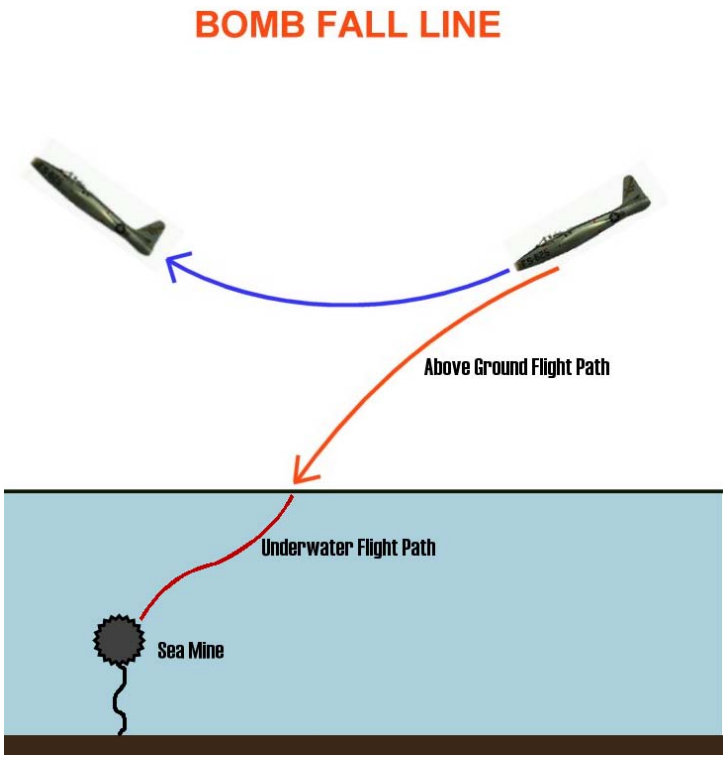

Fig. 1. The concept of airborne sea mine/maritime IED clearance.

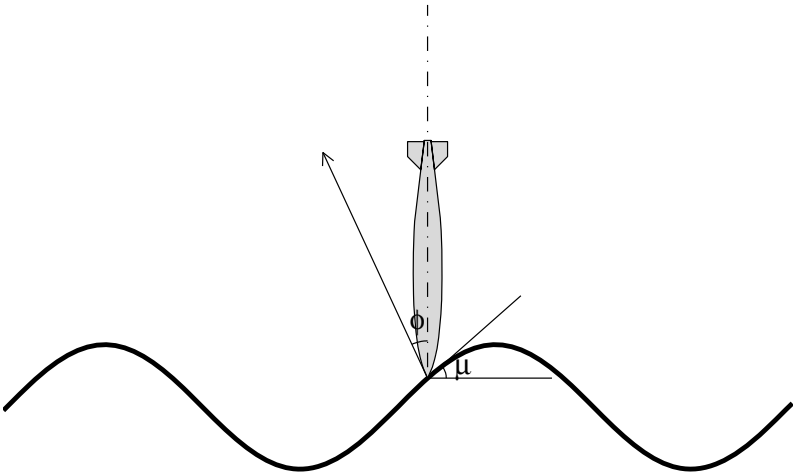

Fig. 2. Ocean surface inclination angle (μ) and bomb impact angle (ϕ) relative to the normal direction of the surface.

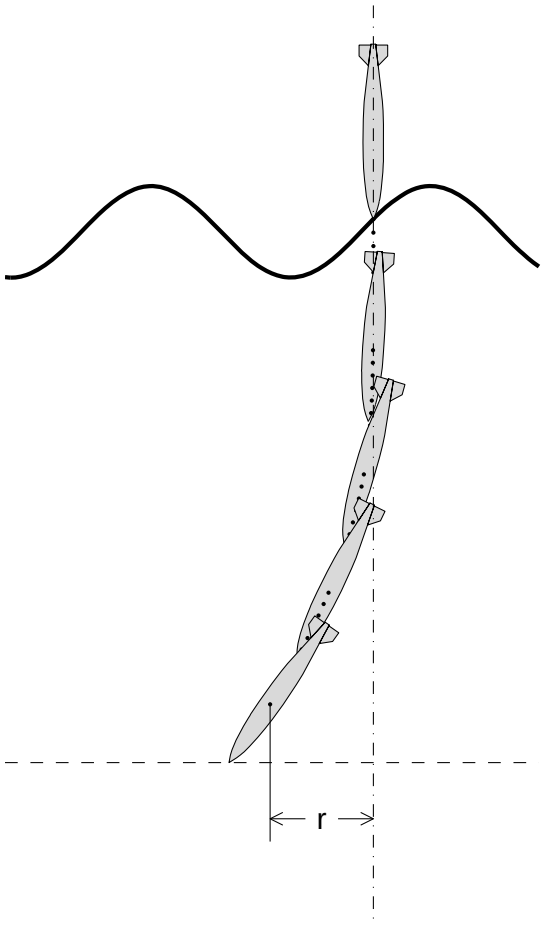

Fig. 3. Dependence of underwater bomb trajectory, orientation, and horizontal deviation (*r*) on the ocean surface slope or on different locations of the waves.

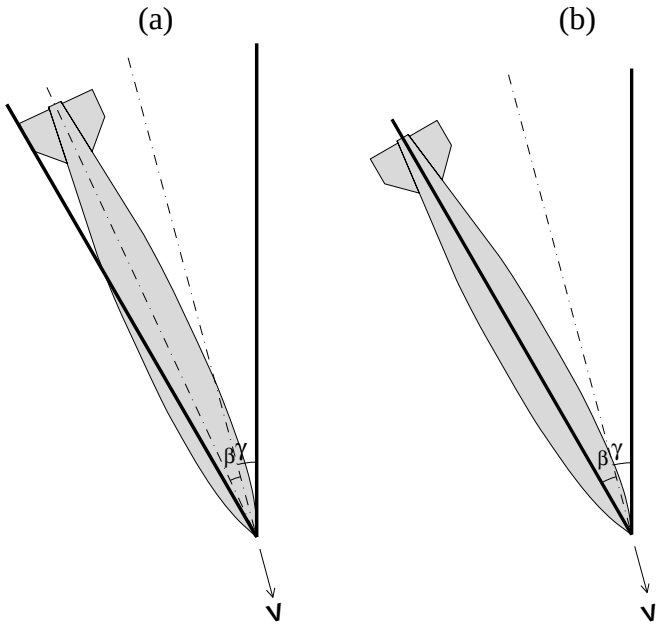

Fig. 4. Air cavity with (a) $\beta < \gamma$ (tail section not hitting the cavity wall, and (b) with $\beta = \gamma$ (tail section hitting the cavity wall).

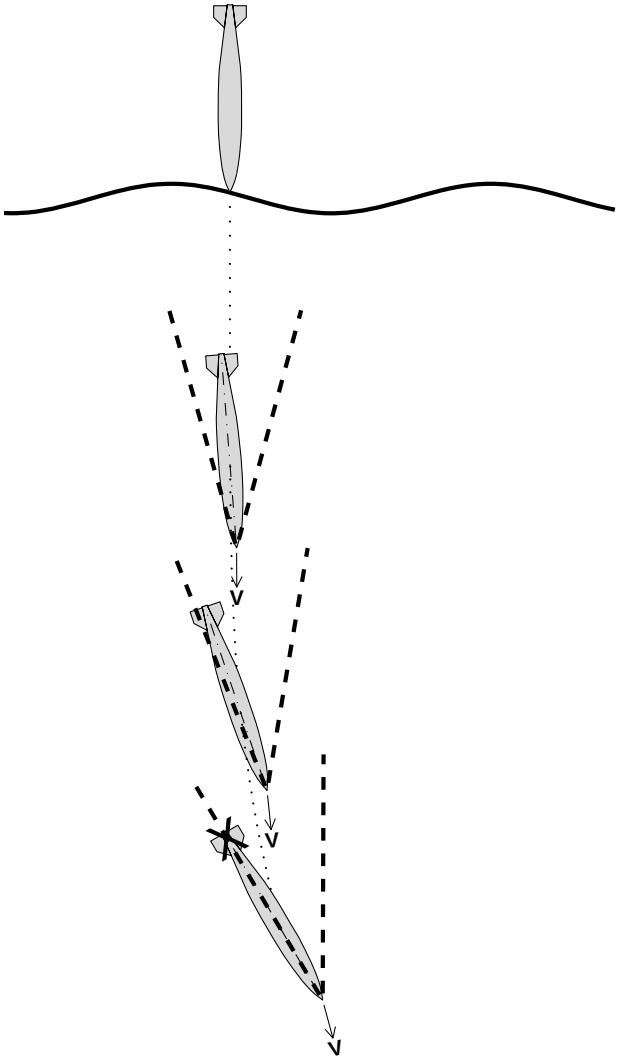

Fig. 5. Wave effect on the air cavity orientation which may cause $\beta > \gamma$ (Tail section hitting the cavity wall).

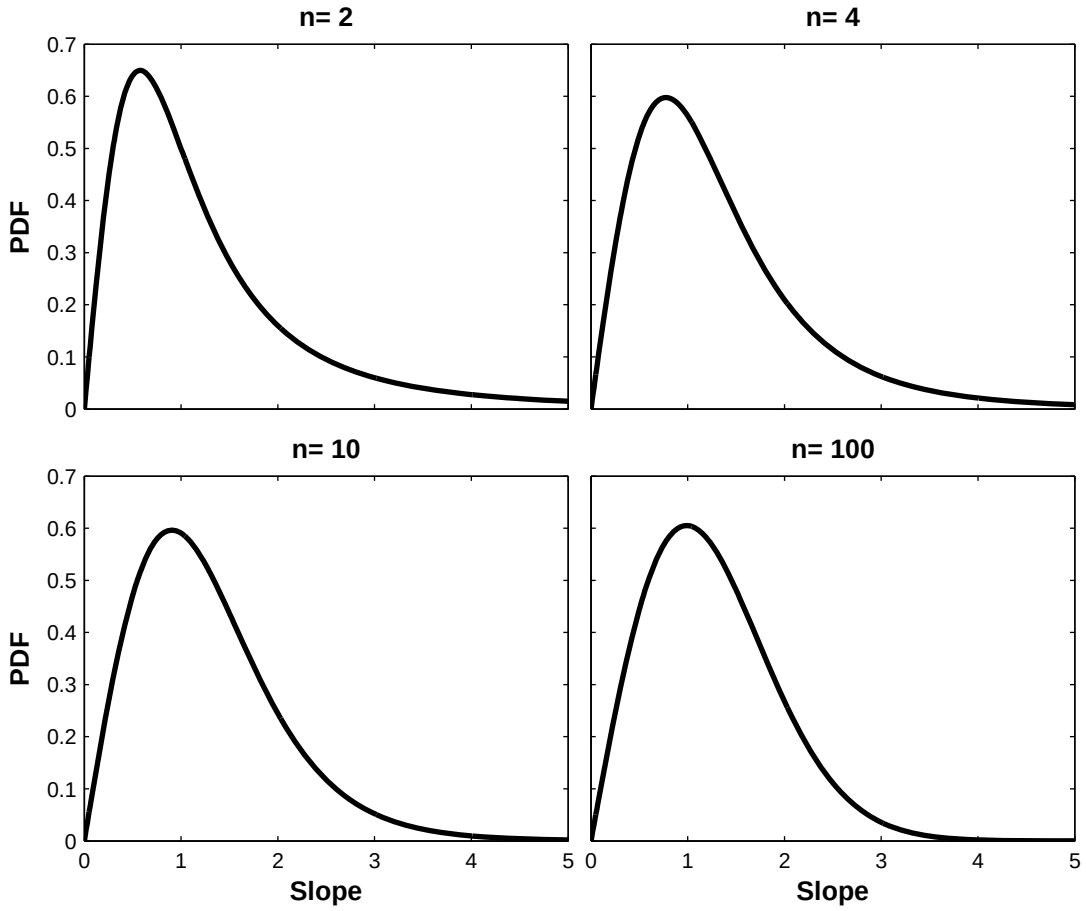

Fig. 6. The s-PDFs for various surface characteristics: (a) n = 2, (b) n = 4, (c) n = 10, and (d) n = 100.

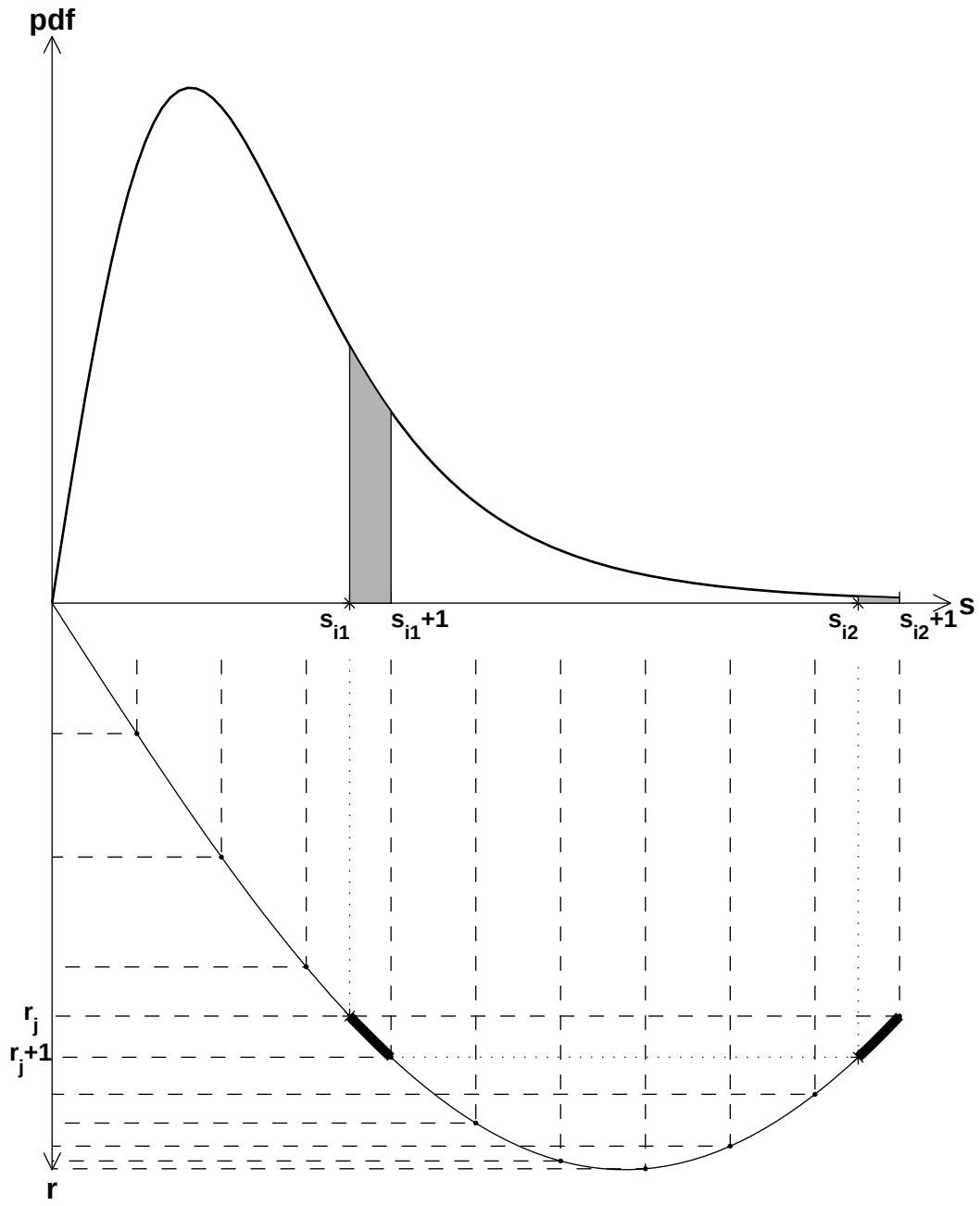

Fig. 7. Calculation of the probability for the bomb's horizontal drift *r* taking values between r_j and r_{j+1} from *m* intervals of surface slope s. Here, *m* = 1, and *m* = 2.

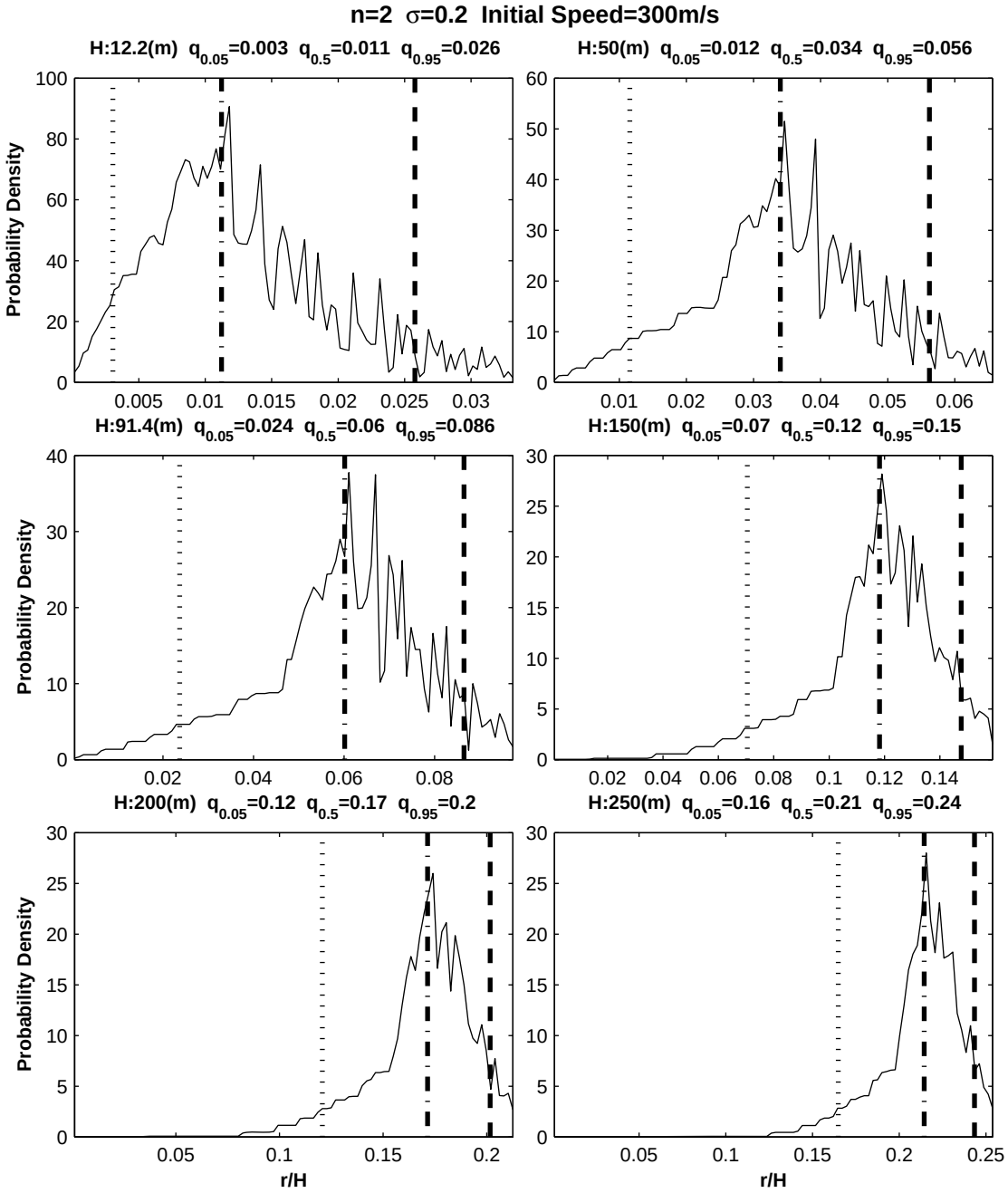

Fig. 8. Probability distribution of the bomb's horizontal drift (scaled by the depth) *r/H* with $n = 2$, $\sigma = 0.2$, and $V = 300$ m/s for various depth: (a) 12.2 m (i.e. 40 ft), (b) 50 m, (c) 91.4 m (i.e., 300 ft), (d) 150 m, (e) 200 m, and (f) 250 m.

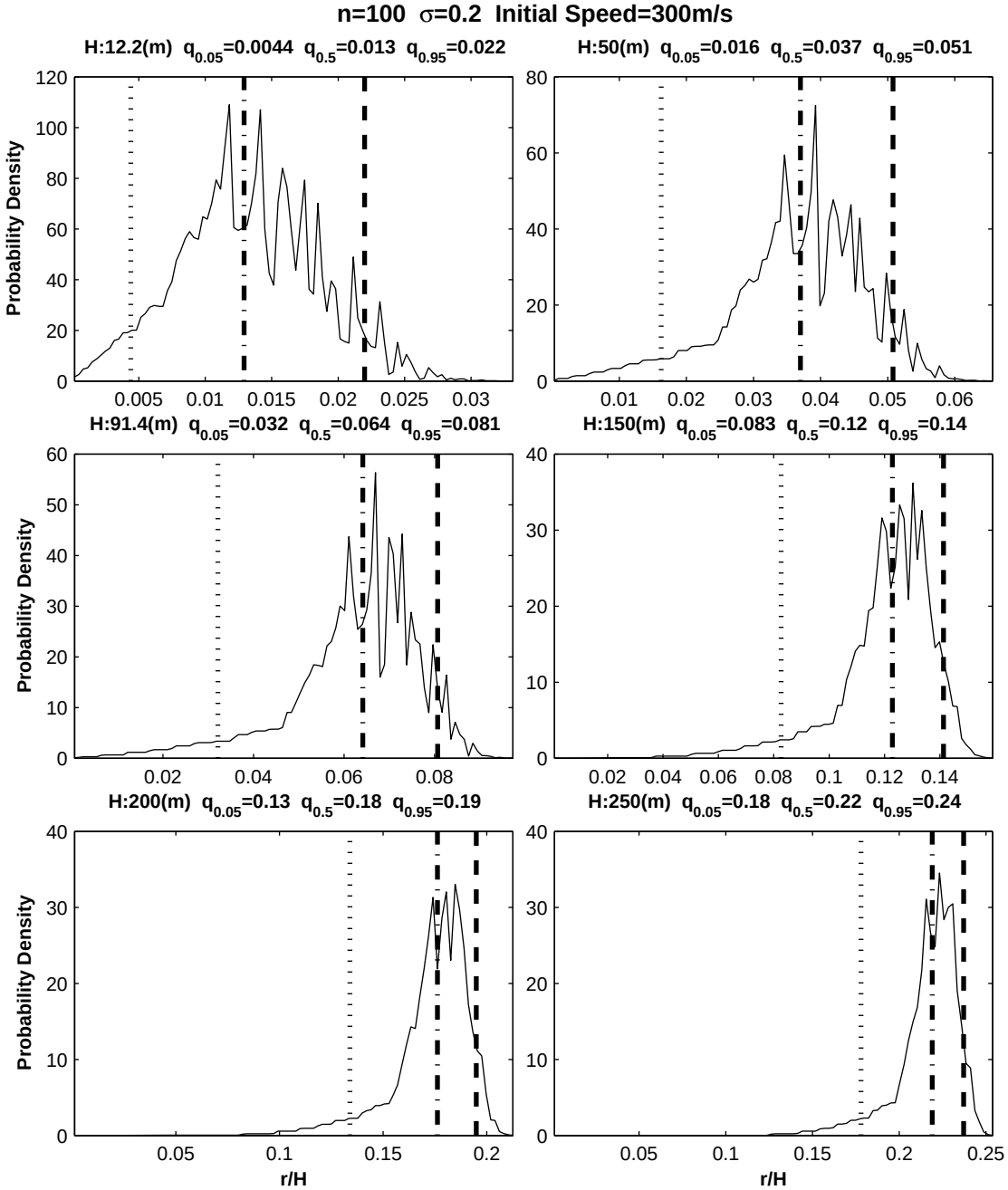

Fig. 9. Probability distribution of the bomb's horizontal drift (scaled by the depth) *r/H* with $n = 100$, $\sigma = 0.2$, and $V = 300$ m/s for various depth: (a) 12.2 m (i.e. 40 ft), (b) 50 m, (c) 91.4 m (i.e., 300 ft), (d) 150 m, (e) 200 m, and (f) 250 m.

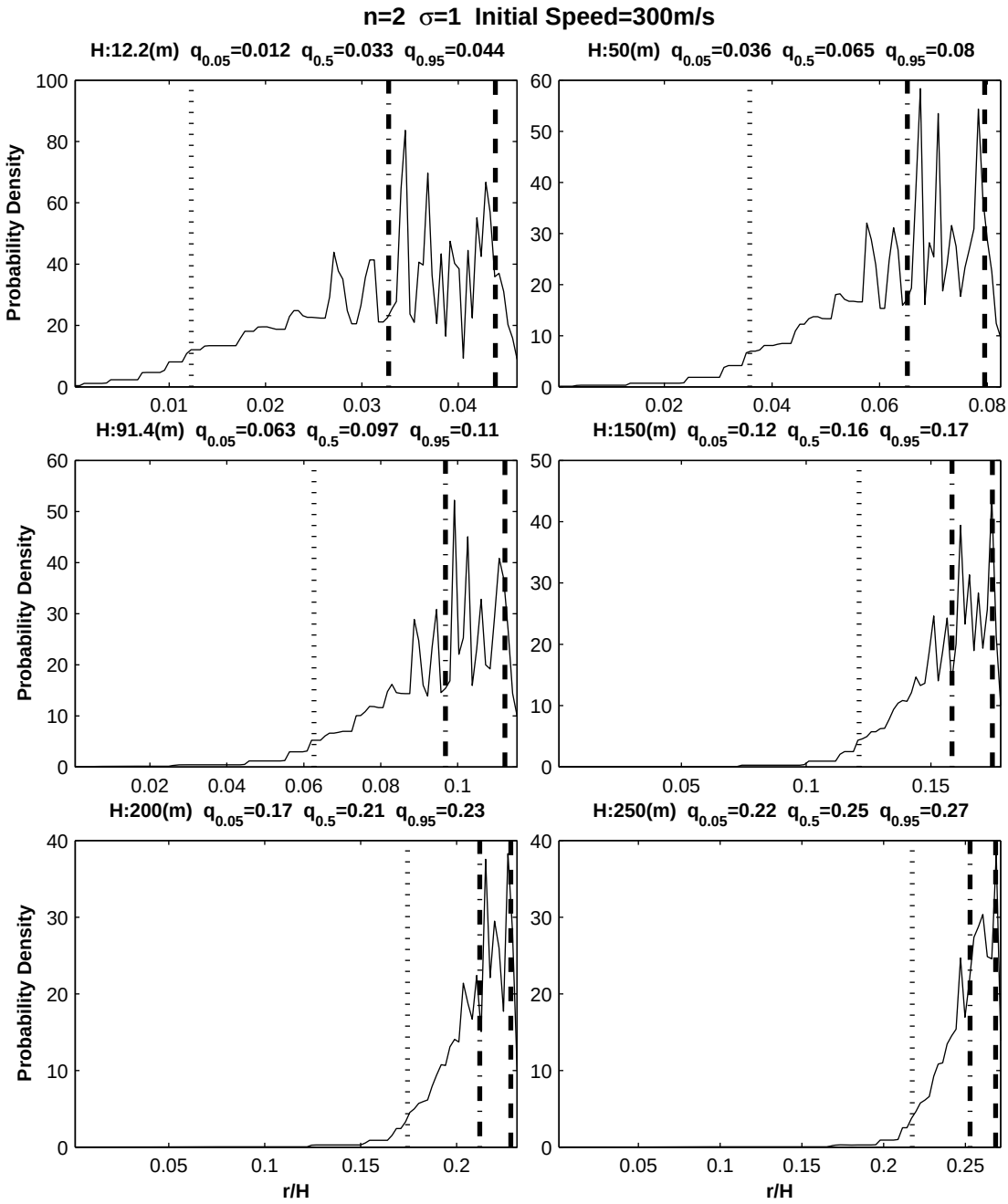

Fig. 10. Probability distribution of the bomb's horizontal drift (scaled by the depth) *r/H* with $n = 2$, $\sigma = 1.0$, $V = 300$ m/s for various depth: (a) 12.2 m (i.e. 40 ft), (b) 50 m, (c) 91.4 m (i.e., 300 ft), (d) 150 m, (e) 200 m, and (f) 250 m.

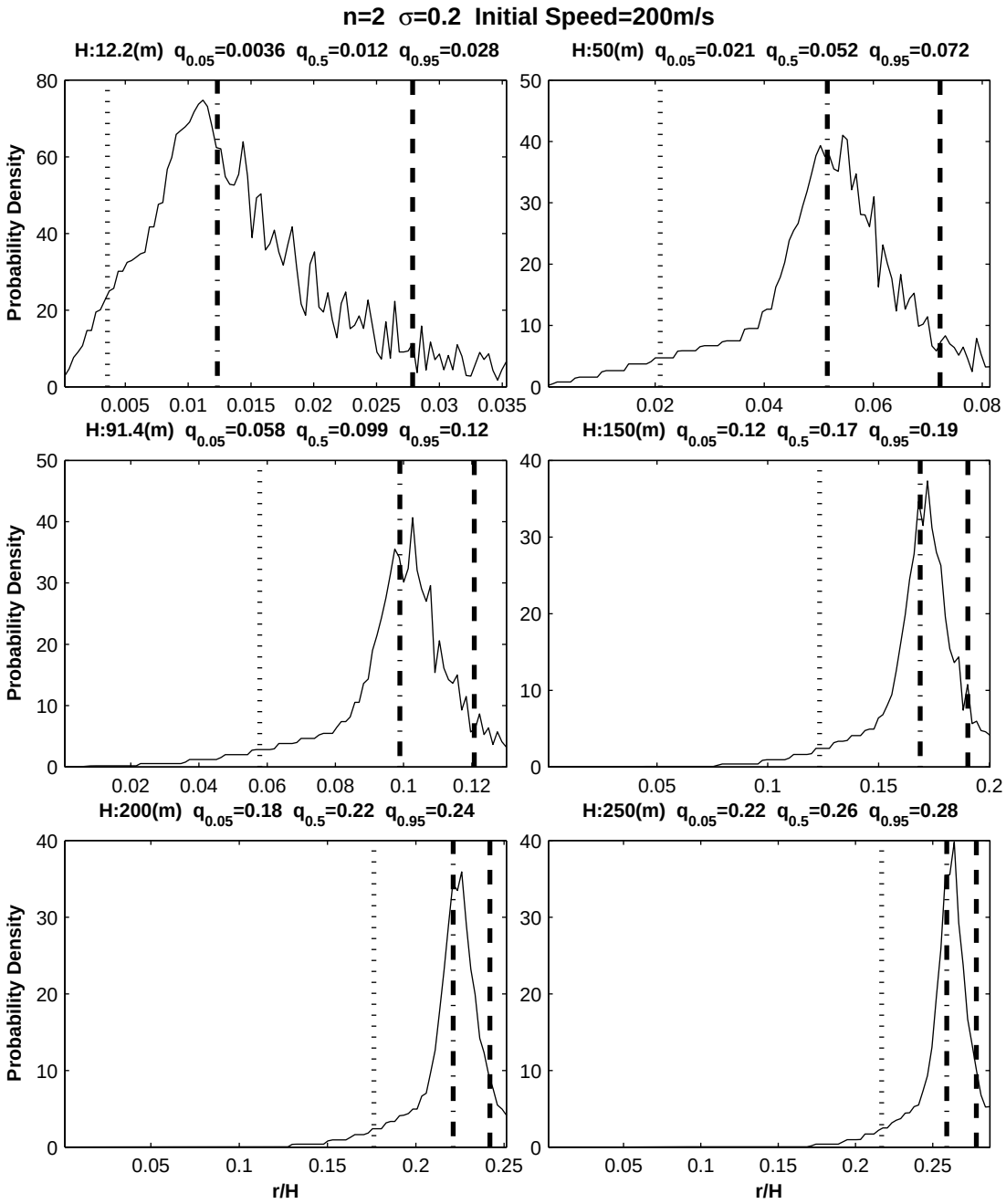

Fig. 11. Probability distribution of the bomb's horizontal drift (scaled by the depth) *r/H* with $n = 2$, $\sigma = 0.2$, $V = 200$ m/s for various depth: (a) 12.2 m (i.e. 40 ft), (b) 50 m, (c) 91.4 m (i.e., 300 ft), (d) 150 m, (e) 200 m, and (f) 250 m.